Title: Mechanism of increased respiration in an H^+-ATPase-defective mutant of *Corynebacterium glutamicum*

Running Title: Increased respiration in *C. glutamicum atp* mutants

Authors: Kazunori Sawada[1], Yui Kato[1], Keita Imai[1], Liyuan Li[1], Masaru Wada[1*], Kazunobu Matsushita[2], and Atsushi Yokota[1]

[1] Laboratory of Microbial Physiology, Research Faculty of Agriculture, Hokkaido University, Kita-9 Nishi-9, Kita-ku, Sapporo, Hokkaido 060-8589, Japan

[2] Department of Biological Chemistry, Faculty of Agriculture, Yamaguchi University, Yamaguchi, Yamaguchi 753-8515, Japan

[*]Corresponding author. Tel: +81-11-706-4185; Fax: +81-11-706-4961.

E-mail address: wada@chem.agr.hokudai.ac.jp (M. Wada).

ABSTRACT

We previously reported that a spontaneous H^+-ATPase-defective mutant of *Corynebacterium glutamicum*, F172-8, derived from *C. glutamicum* ATCC 14067, showed enhanced glucose consumption and respiration rates. To investigate the genome-based mechanism of enhanced respiration rate in such *C. glutamicum* mutants, A-1, a H^+-ATPase-defective mutant derived from *C. glutamicum* ATCC 13032, which harbors the same point mutation as F172-8, was used in this study. A-1 showed similar fermentation profiles to F172-8 when cultured in a jar fermentor. Enzyme activity measurements, quantitative real-time PCR, and DNA microarray analysis suggested that A-1 enhanced malate:quinone oxidoreductase/malate dehydrogenase and L-lactate dehydrogenase/NAD^+-dependent-lactate dehydrogenase coupling reactions, but not NADH dehydrogenase-II, for reoxidation of the excess NADH arising from enhanced glucose consumption. A-1 also up-regulated succinate dehydrogenase, which may result in the relief of excess proton-motive force (pmf) in the H^+-ATPase mutant. In addition, the transcriptional level of cytochrome *bd* oxidase, but not cytochrome bc_1-aa_3, also increased, which may help prevent the excess pmf generation caused by enhanced respiration. These results indicate that *C. glutamicum* possesses intriguing strategies for coping with NADH over-accumulation. Furthermore, these mechanisms are different than those in *Escherichia coli*, even though the two species use similar strategies to prevent excess pmf generation.

INTRODUCTION

Corynebacterium glutamicum, which belongs to the phylum Actinobacteria, is an industrially-important organism for the production of not only various amino acids, including L-glutamic acid and L-lysine (1, 2), but also organic acids such as succinate (3). To develop

effective fermentation processes, a deeper understanding of the fundamental metabolism of this bacterium is required. Whereas numerous studies of the catabolism and anabolism of this bacterium have been performed, the number of reports on its energy metabolism remains limited. In our studies on energy metabolism, we have focused on sugar metabolism in H^+-ATPase-defective mutants of industrially-important bacteria such as *Escherichia coli* and *C. glutamicum* (4, 5, 6). In these H^+-ATPase-defective mutants, energy generation depends on substrate-level phosphorylation, especially that mediated by the glycolytic pathway, because H^+-ATPase plays a main role in oxidative phosphorylation. The most interesting feature of the H^+-ATPase mutants of both *E. coli* and *C. glutamicum* was enhanced glucose metabolism (6, 7). Moreover, the H^+-ATPase defect in both bacteria enhanced the specific respiration rate. These changes are reasonable responses to reoxidize the increased levels of NADH produced by enhanced glucose metabolism.

In a previous study on the mechanisms underlying the enhanced respiratory activity in the H^+-ATPase-defective *E. coli* mutant HBA-1 (5), we discovered intriguing changes in the expression patterns of respiratory chain components, which, to the best of our knowledge, had never before been reported (5). The respiratory chain in *E. coli* consists of NADH dehydrogenase (NDH) and cytochrome oxidase, and *E. coli* possesses several isozymes of both, which differ in their proton-motive force (pmf) generation efficiency: NDH-I ($4H^+/2e^-$), NDH-II ($0H^+/2e^-$), cytochrome bo_3 oxidase ($4H^+/2e^-$), cytochrome *bd*-I (Cyt *bd*-I) ($2H^+/2e^-$), and cytochrome *bd*-II ($0H^+/2e^-$). The *atp* mutation resulted in specific up-regulation of less efficient pmf generation components, such as NDH-II and Cyt *bd*-I. These alterations are a reasonable strategy to avoid generating excess pmf in the H^+-ATPase-defective *E. coli* mutant during increased respiration.

On the other hand, in the H^+-ATPase-defective *C. glutamicum* mutant, the mechanism of

enhanced respiration remains unknown, even though the respiratory chain components of this bacterium are well described. Unlike *E. coli*, *C. glutamicum* possesses only NDH-II, which is not coupled to pmf generation (8), and two isozymes of cytochrome oxidases, i.e., cytochrome bc_1-aa_3 supercomplex (9) and cytochrome *bd* oxidase (10, 11), which have different pmf generation efficiencies. *C. glutamicum* possesses other respiratory components, such as membrane-bound malate:quinone oxidoreductase (MQO, (8, 12)) and L-lactate dehydrogenase (LldD, (13)), which transfer electrons to the respiratory chain using menaquinone as the primary electron acceptor. MQO and LldD have been shown to function as unique NADH reoxidation systems when coupled to the reverse reactions catalyzed by soluble NAD^+ dependent-malate dehydrogenase (MDH) and soluble NAD^+ dependent-lactate dehydrogenase (LdhA), respectively, in *in vitro* experiments (8, 13). The LldD/LdhA coupling reaction was previously reported to compensate for the ability of an NDH-II-gene (*ndh*)-disruption mutant to reoxidize NADH (13). This coupling reaction was also assumed to function as an NADH reoxidation system under anaerobic conditions with nitrate (14). However, there has been no report on the physiological role of these unique NADH reoxidation systems *in vivo*, and the physiological roles of these cytochrome oxidases remain to be clarified.

In a comparative proteome analysis of *C. glutamicum* ATCC 14067 (wild-type, formerly known as *Brevibacterium flavum* No. 2247) and its spontaneous H^+-ATPase-defective mutant, F172-8 (which has a point mutation in *atpG*, a gene that encodes the gamma subunit of F_1-ATPase), we found simultaneous up-regulation of MQO and MDH in the latter (15). This suggested that the enhanced NADH reoxidation mediated by the MQO/MDH coupling reaction might explain the increased respiration rate in the H^+-ATPase-defective mutant, suggesting the physiological importance of the MQO/MDH coupling reaction in respiration. Because *C. glutamicum* possesses

respiratory components other than MQO/MDH, additional changes that contribute to the enhanced respiration were also expected. However, because of the technical difficulty of proteomic detection of membrane-associated enzymes, the detailed mechanism of enhanced respiration remains unclear.

In this study, to investigate the genome-based mechanism underlying the increased respiration found in the H^+-ATPase-defective mutant, we used another set of strains: *C. glutamicum* ATCC 13032 (wild-type), the complete genome sequence of which is available, and its defined H^+-ATPase-defective mutant strain A-1 (16), which possesses the same point mutation as F172-8. Both the A-1 and F172-8 mutants exhibited elevated activities of MQO/MDH coupling reactions, and mechanisms other than those previously reported in *E. coli* H^+-ATPase-defective mutants were identified. This study provides not only clues to both the physiological role and transcriptional regulation of respiratory chain components *in vivo* but also important information that will facilitate the biotechnological application of this bacterium.

MATERIALS AND METHODS

Bacterial strains The *C. glutamicum* strains used in this study are listed in Table 1. F172-8 was obtained as a spontaneous neomycin-resistant mutant from *C. glutamicum* ATCC 14067. The defined H^+-ATPase-defective mutant strain A-1 was derived from *C. glutamicum* ATCC 13032 by introducing the same point mutation (S237P) as in F172-8 by double-crossover replacement (16).

Media The complete medium, Medium 7 (6), contained (per liter) 10 g of Polypepton (Nihon Pharmaceutical Co., Ltd., Tokyo), 10 g of yeast extract (Nacalai Tesque, Inc., Kyoto), 5 g of NaCl, 5 g of glucose, and NaOH to adjust the pH to 7.0. When necessary, 20 g of agar was added to

solidify the medium, and filter-sterilized neomycin solution was added to a final concentration of 1 or 2 mg/L. The seed medium for the fermentation analysis was Medium S2, containing 60 μg of biotin (6). As the jar fermentation medium, either the complex Medium F4 supplemented with 60 μg/L biotin (15) or the semisynthetic Medium G3 was used. Medium G3 contained (per liter) 50 g of glucose, 25 g of $(NH_4)_2SO_4$, 1.0 g of KH_2PO_4, 1.0 g of $MgSO_4 \bullet 7H_2O$, 0.01 g of $FeSO_4 \bullet 7H_2O$, 0.01 g of $MnSO_4 \bullet 7H_2O$, 200 μg of thiamine•HCl, 60 μg of biotin, and 1.4 mL of soybean-meal hydrolysate (total nitrogen 35 g/L).

Culture conditions *C. glutamicum* ATCC 14067 and F172-8 were cultured at 30°C as described previously (15). Briefly, strains were refreshed on Medium 7 for 48 h; the medium was supplemented with 1 mg/L neomycin for F172-8. Strains were then precultured in 20 mL of Medium S2 in 500 mL shaking flasks until the early stationary phase, i.e., 10 h for ATCC 14067 and 14 h for F172-8. The cells were harvested by centrifugation, washed twice with 0.9% NaCl, and resuspended in the same solution. Washed cells were inoculated into 1.2 L Medium F4 to an initial OD 660 of 1.0 in a 2 L jar fermentor (BMJ-02PI, ABLE Corp., Tokyo). Cultures were aerated at 1 vvm with stirring at 750 rpm. The pH was maintained at 7.0 using a 28% (w/w) ammonia solution.

For *C. glutamicum* ATCC 13032 and its H^+-ATPase-defective mutant A-1, cells were refreshed twice on Medium 7 agar plates for 24 h (ATCC 13032) or 48 h (A-1); Medium 7 for A-1 was supplemented with 2 mg/L (for first refresh) and 1 mg/L (for second refresh) neomycin. Then two successive precultures were conducted in Medium S2, first in 5 mL of medium in a test tube for 12 h and then in 200 mL of medium in 2 L shaking flasks until the early stationary phase, i.e., 10 h for ATCC 13032 and 13 h for A-1. The cells were washed by the same method as ATCC 14067 and

F172-8 and inoculated into 1.2 L of Medium G3 in a 2 L jar fermentor to an initial OD 660 of 1.0. Jar fermentation was conducted under the same conditions as used for ATCC 14067 and F172-8, except that a DO stat culture was applied, wherein the level of dissolved oxygen was maintained above 2 ppm by maintaining the agitation speed between 750 and 980 rpm, and the pH was maintained at 7.0 with 5 N NaOH.

Analytical methods Growth, residual glucose, and respiration rate were measured as described previously (6). The average rate of glucose consumption per cell was calculated as [decreased glucose (g/L)] [increased dry cell (mg/L)]$^{-1}$ h^{-1}. Respiration rate was expressed as (mmol O_2 consumed) min^{-1} (mg dry cell weight)$^{-1}$. The dry cell weight of ATCC 13032 and A-1 was calculated from the correspondence of one optical density unit at 660 nm to 0.360 mg and 0.400 mg dry cell weight per mL, respectively. Extraction of intracellular NAD^+ and NADH were performed as described by Inui et al. (17). Briefly, cells cultured to the exponential phase in Medium G3 in 2 L jar fermentors were harvested by centrifugation at 20,400 × *g* at 4°C for 1 min. For NAD^+ extraction, the cells were resuspended in 2.5 N HCl containing 50% ethanol and then heated at 55°C for 8 min. After cooling on ice, the mixture was neutralized with KOH. For NADH extraction, the cells were resuspended in 3 N KOH containing 50% ethanol and then heated at 55°C for 5 min. After cooling on ice, the mixture was neutralized with HCl. The extracts were centrifuged at 20,400 × *g* at 4°C for 5 min to remove cell debris, and supernatants were kept at −20°C until use. Measurement of intracellular NAD^+ and NADH concentrations was conducted using the cycling assay (18, 19) within 24 h of extraction. Assay mixture (total volume, 1.0 mL) contained 300 mM Bicine buffer (pH 8.0), 4 mM EDTA, 0.42 mM 3-(4,5-dimethylthiazol-2-yl)-2,5-diphenyltetrazolium bromide, 3.32 mM phenazine ethosulfate, 100

μL of absolute ethanol, alcohol dehydrogenase (15 U for NAD^+ or 30 U for NADH), and 50 μL of cell extract. Intracellular concentrations were calculated by assuming the intracellular volume to be 1.5 μL (mg dry cell weight)$^{-1}$.

Enzyme assays Cells cultured to the exponential phase in Medium F4 or Medium G3 in 2 L jar fermentors were harvested by centrifugation, washed twice with 0.2% KCl solution, and kept at –80°C until use. The cells were resuspended in an appropriate extraction buffer for each enzyme assay, and then disrupted three times using a French Pressure Cell (Ohtake Works, Tokyo) at 110 MPa. Cell debris was removed by centrifugation at 10,000 × *g* at 4°C for 10–20 min. The supernatant was ultracentrifuged at 75,000 × *g* at 4°C for 60–90 min. For MQO, LldD, succinate dehydrogenase (SDH), NADH dehydrogenase (NDH-II), and *N,N,N',N'*-tetramethyl-*p*-phenylenediamine (TMPD) oxidase assays, the pellet was resuspended by homogenization with a micro homogenizer in the appropriate suspension buffer; this was used as the crude enzyme. For MDH and LdhA assays, the supernatants were filtered through a PD-10 column (GE Healthcare UK Ltd., Buckinghamshire, UK) using an appropriate extraction buffer to remove low-molecular-weight contaminants and the eluate was used as the crude enzyme.

All enzyme activity assays were conducted using 1 mL reaction mixture at room temperature (25°C). For the MQO, LldD, and SDH assays, 50 mM HEPES buffer (pH 7.5) containing 10 mM CH_3COONa, 10 mM $CaCl_2$, and 5 mM $MgCl_2$ was used as the extraction and suspension buffer. The reaction mixture contained an appropriate amount of enzyme, 50 mM HEPES buffer (pH 7.5), 10 mM CH_3COONa, 50 mM Vitamin K_3, 50 mM 2,6-dichloroindophenol (DCIP), 10 mM FAD, and 1 mM substrate (L-malate, L-lactate, or succinate). MQO, LldD, and SDH activities were measured spectrophotometrically by following the change in the absorbance of

DCIP at 600 nm (8). A value of 22 for the millimolar extinction coefficient of DCIP was used to calculate the specific activity.

For the NDH-II and TMPD oxidase assays, 20 and 50 mM potassium phosphate buffer (pH 7.5) were used as the extraction and suspension buffers, respectively. NDH-II was determined spectrophotometrically by measuring the change in the absorbance of NADH at 340 nm (13). The reaction mixture consisted of 50 mM potassium phosphate buffer (pH 7.5), 20 mM FAD, 0.2 mM NADH, and an appropriate amount of enzyme. A value of 6.3 for the millimolar extinction coefficient of NADH was used to calculate the specific activity. TMPD oxidase was determined spectrophotometrically by measuring the change in the absorbance of TMPD, an artificial electron donor, at 520 nm (13). The reaction mixture consisted of 30 mM MOPS-NaOH buffer (pH 7.0), 2.0 mM TMPD, 1.0 mM EDTA, and an appropriate amount of enzyme. A value of 6.1 for the millimolar extinction coefficient of TMPD was used to calculate the specific activity.

For MDH and LdhA assays, 20 mM potassium phosphate buffer (pH 7.5) was used as the extraction buffer. MDH and LdhA were monitored spectrophotometrically by measuring the changes in the absorbance of NADH at 340 nm (13). The reaction mixture consisted of 50 mM potassium phosphate buffer (pH 7.5 and pH 7.0 for MDH and LdhA assays, respectively), 0.2 mM NADH, 10 mM substrate (oxaloacetate for MDH or pyruvate for LdhA), and an appropriate amount of enzyme. A value of 6.3 for the millimolar extinction coefficient of NADH was used to calculate the specific activity. The protein concentration of crude extracts was determined with a Bio-Rad Protein Assay kit (Bio-Rad Laboratories, Inc., Hercules, CA, USA) with bovine serum albumin as the standard. When the membrane fraction was used as the enzyme, an equal volume of 0.4% Triton X-100 was added to solubilize membrane proteins. The specific activity of each enzyme was

expressed as nmol min^{-1} (mg protein)$^{-1}$.

Quantitative real-time PCR analysis Total RNA extraction, cDNA synthesis, and quantitative real-time PCR were performed as described previously (20). The sequences of the forward primers, fluorogenic primers labeled with FAM (6-carboxy-fluorescein) as a reporter dye, and reverse primers for target genes are listed in Table 2. The 16S rRNA gene was used as an endogenous control. Each sample was analyzed in at least duplicate. A relative standard curve method was used to calculate the relative expression level of the target genes. The expression ratio was obtained by dividing the relative expression level of the mutant by that of the wild-type strain.

DNA microarray analysis Arrays were designed to cover all 6,040 predicted open reading frames (ORFs) of *C. glutamicum* ATCC 13032 (NC_003450 and NC_006958). On average, five replicate probes (60-mers) were designed for each ORF. Synthesis of cDNA from total RNA (extracted as described above), labeling of cDNA with Cy3, hybridization, and scanning were performed using Roche NimbleGen. Data extraction and normalization by the robust multiarray average (RMA) procedure were conducted by Roche NimbleGen according to the standard method. Analysis was conducted using total RNA extracted from two independent cultures, and hybridization was conducted in duplicate.

The raw microarray data are available at http://cibex.nig.ac.jp/ with CIBEX accession no. CBX191.

RESULTS

Fermentation analysis The fermentation profiles of the wild-type ATCC 13032 and its mutant A-1 in semisynthetic Medium G3 were similar to those of wild-type ATCC 14067 and its mutant F172-8 in Medium F4 (a complex medium, as described in a previous report (15)), such that

the mutant exhibited slower rates of growth (Fig. 1A) and glucose consumption (Fig. 1B) than the wild-type. Although A-1 showed less glucose consumption, the specific glucose consumption rate during exponential growth, which was calculated as [decreased glucose (g/L)] [increased dry cell (mg/L)]$^{-1}$ h^{-1} for cultures (using data between 9 and 12 h) was twice that of ATCC 13032 (calculated using data between 4.5 and 7.5 h; Table 3). This difference was maintained even if the specific glucose consumption rate was calculated with data obtained from any sampling point during exponential growth phase. Furthermore, strain A-1 exhibited a 1.4-fold increased specific respiration rate compared to ATCC 13032 (Table 3). These profile shifts are similar to those observed in ATCC 14067 and F172-8 cultured in Medium F4 (15). These data suggest that the defined H^+-ATPase-defective mutant A-1 exhibited comparable metabolic changes in semisynthetic Medium G3 to those of F172-8 cultured in complex Medium F4, i.e., enhanced glucose consumption and respiration.

Enzyme activity measurements To elucidate the metabolic changes associated with enhanced respiration, the specific activities of enzymes involved in respiration and NADH reoxidation were measured. Figure 2A shows the activities of MQO, MDH, LldD, LdhA, and NDH-II in ATCC 14067 and F172-8 exponential-phase cells growing in Medium F4. In our previous comparative proteome analysis (15), the expression of the MQO/MDH coupling reaction, which functions as an NADH reoxidation system (8), was elevated in F172-8 compared to ATCC 14067. Similarly, the activities of MQO and MDH were 3.0- (with statistic significance) and 2.0-fold (without statistic significance) higher in F172-8 than in ATCC 14067, respectively. Interestingly, the activities of LldD and LdhA, which also contribute to NADH reoxidation (13), were up-regulated 4.6- and 2.4-fold in F172-8 compared to ATCC 14067, respectively, both with

statistic significance. On the other hand, the activity of NADH dehydrogenase (NDH-II), which is the main entry site for NADH from the central metabolism to the respiratory chain in most organisms, did not differ between ATCC 14067 and F172-8.

Similar changes, including increased MQO/MDH and LldD/LdhA coupling reaction activities and no difference in NDH-II activity, were observed in ATCC 13032 and A-1 cultured in Medium G3 (Fig. 2B). Furthermore, SDH activity, which catalyzes conversion of succinate to fumarate in the TCA cycle and transfers electrons into the respiratory chain using menaquinone, was significantly higher (2.4-fold) in A-1 than in ATCC 13032. Thus, all of these phenotypes are likely intrinsically associated with the *atp* mutation in *C. glutamicum*, irrespective of differences in strain background. The observed up-regulated activities of the two coupling reactions (MQO/MDH and LldD/LdhA) and the increased SDH activity seem to contribute to the increased specific respiration rate in the H^+-ATPase mutant strain A-1.

To determine whether these alterations were accompanied by changes in transcriptional level, DNA microarray and quantitative real-time PCR were performed using total RNA extracted from ATCC 13032 and A-1 harvested during exponential growth. As shown in Table 4, and corresponding to changes in enzyme activities, the transcription levels of genes encoding MDH, LldD and LdhA were significantly up-regulated, those encoding MQO and SDH showed tendencies of up-regulation compared to ATCC 13032, but that of NDH-II was unchanged. These results suggest that the increased activities of these enzymes, especially MDH, LldD and LdhA, were regulated at the transcriptional level.

Terminal oxidase analysis The up-regulated activities of menaquinone-reducing enzymes such as MQO, LldD, and SDH observed in A-1 (Fig. 2B) suggested concomitant changes

in terminal oxidase activity. Two types of terminal oxidase, which have different pmf generation efficiencies, have been found in the *C. glutamicum* respiratory chain: cytochrome bc_1-aa_3 supercomplex ($6H^+/2e^-$) and cytochrome *bd* oxidase ($2H^+/2e^-$). To estimate terminal oxidase activity, we measured the total activity as TMPD oxidase activity. As shown in Fig. 2B, TMPD oxidase activity of A-1 was 2.5-fold higher than that of ATCC 13032. The transcriptional levels of the genes encoding terminal oxidases were also determined by DNA microarray and quantitative real-time PCR. As shown in Table 4, the DNA microarray results suggest preferential increases in the transcription of genes encoding cytochrome *bd* oxidase (*cydAB*) but not the cytochrome bc_1-aa_3 supercomplex (*qcrCAB*, *ctaCD*). Quantitative real-time PCR analysis confirmed that the transcriptional level of cytochrome *bd* oxidase (*cydAB*) was significantly increased, but that of cytochrome bc_1-aa_3 supercomplex (*ctaC*) was unchanged in A-1 compared to ATCC 13032. The results of the terminal oxidase activity measurement, DNA microarray, and quantitative real-time PCR analyses indicate that the increased total terminal oxidase activity resulted from the preferential increase in cytochrome *bd* oxidase activity.

Intracellular concentrations of NAD^+ and NADH In the H^+-ATPase-defective mutant A-1, enhanced respiration aided by the increased activities of two coupling reactions (MQO/MDH and LldD/LdhA) and the terminal oxidase (most likely cytochrome *bd* oxidase) was evident. To investigate whether these changes aid in coping with the increased NADH generated by enhanced glucose metabolism, the intracellular NAD^+ and NADH concentrations in ATCC 13032 and A-1 growing exponentially in Medium G3 were measured. As shown in Table 5, although the total concentration of NADH-related compounds are not identical in the two strains (probably due to the difference of extraction efficiency), the NAD^+/NADH ratio decreased from 13.0 in ATCC

13032 to 5.42 in A-1, suggesting that in the H^+-ATPase mutant, NADH reoxidation remained inadequate compared to ATCC 13032.

DISCUSSION

The present study clarifies the overall changes in respiratory chain components in H^+-ATPase-defective mutants of *C. glutamicum* ATCC 14067 and ATCC 13032 (Fig. 3). The results illustrate the interesting mechanism that this bacterium employs to increase respiration as a result of the enhanced glucose metabolism caused by the H^+-ATPase defect.

The defined H^+-ATPase-defective mutant strain, A-1, showed increased specific glucose consumption and respiration rates (Table 3) during culture in semisynthetic Medium G3. Increased glucose consumption may cause over-accumulation of intracellular NADH, which is generated by glycolysis and the TCA cycle. In fact, measurement of the intracellular NAD^+ and NADH concentrations revealed an accumulation of NADH in A-1 (Table 5). Enzyme activity measurement (Fig. 2) and transcriptional analysis (Table 4) indicated up-regulated activity of two coupling reactions, MQO/MDH and LldD/LdhA, which are known to be involved in NADH reoxidation in *C. glutamicum* (8, 13). Therefore, these findings demonstrate a physiological role of both the MQO/MDH and LldD/LdhA coupling reactions in the facilitation of reoxidation of over-accumulated NADH in the H^+-ATPase-defective mutant (Table 5). Surprisingly, the activity and transcriptional level of NDH-II, which is the main NADH reoxidation enzyme in many microorganisms, did not significantly increase (Fig. 2 and Table 4), even though the NAD^+/ NADH ratio in A-1 was lower than that in ATCC 13032. Taken together, these results indicate that both the MQO/MDH and LldD/LdhA coupling reactions, but not NDH-II, facilitate increased NADH reoxidation in the H^+-ATPase-defective mutant.

SDH, which is a membrane-integral enzyme, transfers electrons to menaquinone while importing protons from the periplasmic space across the cytoplasmic membrane (21, 22) during the conversion of succinate to fumarate. SDH activity was also up-regulated in the mutant (Fig. 2), although it does not directly contribute to NADH reoxidation. SDH may function to relieve the over-accumulation of protons in the periplasmic space that was derived from enhanced respiration and the inability of oxidative phosphorylation to consume pmf in the H^+-ATPase-defective mutants.

In terms of terminal oxidase, a series of analyses (enzyme activity measurement, DNA microarray experiments, and quantitative real-time PCR) demonstrated specific up-regulation of cytochrome *bd* oxidase ($2H^+/2e^-$) but not cytochrome bc_1-aa_3 oxidase ($6H^+/2e^-$) (Table 4), suggesting that A-1 avoids excess pmf generation while enhancing respiration.

It is interesting to note that while activation of glucose consumption and increased respiratory activity were also observed in the H^+-ATPase-defective *E. coli* mutant HBA-1 (5), its strategy to prevent NADH over-accumulation differed from that of *C. glutamicum* (Table 6). Whereas strain A-1 did not show significant down-regulation of transcription in genes involved in the TCA cycle (data shown in CIBEX database), the *E. coli* mutant limits the TCA cycle flux to avoid the formation of excess NADH (5). In addition, the *E. coli* mutant enhances NADH reoxidation by preferentially increasing the activities of both NDH-II and cytochrome *bd* oxidase (5). Both of these enzymes have lower pmf generation efficiencies than their counterparts. These differences in strategy suggest that the *C. glutamicum* mutant relies on the entry site of NADH recycling in the TCA cycle (MQO/MDH) or glycolysis (LldD/LdhA) enzymes more than normal respiratory chain enzymes, such as NADH dehydrogenase. These intriguing preferences may reflect the robustness of central metabolism in *C. glutamicum*. The changes in the respiratory components

of both *C. glutamicum* and *E. coli* seem to be reasonable strategies for enhancing respiration while avoiding the generation of excess pmf. These changes may also decrease the potential electron transfer back pressure formed by excess generation of pmf (23) and thus enable smooth increases in the respiration rate.

The transcriptional regulators of *C. glutamicum* have been studied extensively. Several global regulators are known to regulate the transcription of genes that are altered in the H^+-ATPase mutant (Table 4) (24). RamA has been reported to regulate *mqo*, *sdhA*, *lldD*, and *ldhA* transcription (25-27); RamB has been reported to regulate *mdh* and *sdhA* transcription (28); and GlxR has been reported to be responsible for *sdhA*, *lldD*, and *ldhA* transcription regulation (25, 29, 30). The transcriptional regulator of *cydA* and *cydB* has not yet been reported. Because complete illustration of the transcriptional regulation mechanism has not yet been achieved and the role of some global regulators such as GlxR have not been fully clarified (29, 30), only *lldD* and *ldhA* transcriptional regulation are discussed in this study. The transcription of *ldhA* is reported to be repressed by the global transcriptional regulator SugR (31), which was originally identified as a transcriptional regulator of genes involved in the phosphotransferase system (32, 33). Fructose 1-phosphate and fructose 1,6-bisphosphate have been reported as negative effectors of SugR for *ldhA* transcriptional repression (34, 35). The increased glucose consumption rate in A-1 may cause higher intracellular concentrations of fructose 1,6-bisphosphate, which is a glycolysis intermediate. Consequently, transcriptional repression of *ldhA* by SugR is expected to become inactivated, leading to enhanced lactate formation. In addition, *lldD* and *ldhA* are transcriptionally negatively regulated by LldR, another global transcriptional regulator (36, 37). LldR loses its DNA binding ability in the presence of L-lactate (36, 37). Therefore, enhanced transcription of LldD/LdhA may be caused by release

from transcriptional repression by SugR and LldR under the enhanced glycolytic flux and intracellular lactate concentration in the mutants.

In conclusion, we report a unique mechanism of increased respiration in H^+-ATPase-defective mutants of *C. glutamicum*. As shown in Fig. 3, to cope with excess intracellular NADH, the H^+-ATPase-defective mutant increased the activities of the MQO/MDH and LldD/LdhA coupling reactions for NADH reoxidation and cytochrome *bd* oxidase to complete electron transfer to oxygen, which are all suggested to be regulated at the transcriptional level. The choice of the *bd*-type oxidase is reasonable to avoid the excess formation of pmf that would otherwise result from increased respiration. We also observed higher SDH activity in the mutant, which may relieve excess pmf accumulation. Furthermore, we discussed the changes in the transcriptional level of respiration-related enzymes in light of the roles of several recently reported *C. glutamicum* transcriptional regulators. These data contribute to a deeper understanding of the physiology of *C. glutamicum* and will facilitate more efficient production of metabolites by this bacterium.

REFERENCES

1. **Eggeling, L. and Sahm, H.:** L-Glutamate and L-lysine: traditional products with impetuous developments. Appl. Microbiol. Biotechnol., **52,** 146-153 (1999).

2. **Hermann, T.:** Industrial production of amino acids by coryneform bacteria. J. Biotechnol., **104,** 155-172 (2003).

3. **Okino, S., Noburyu, R., Suda, M., Jojima, T., Inui, M., and Yukawa, H.:** An efficient succinic acid production process in a metabolically engineered *Corynebacterium glutamicum* strain. Appl. Microbiol. Biotechnol., **81,** 459-464 (2008).

4. **Aoki, R., Wada, M., Takesue, N., Tanaka, K., and Yokota, A.:** Enhanced glutamic acid production by a H^+-ATPase-defective mutant of *Corynebacterium glutamicum*. Biosci. Biotechnol. Biochem., **69,** 1466-1472 (2005).

5. **Noda, S., Takezawa, Y., Mizutani, T., Asakura, T., Nishiumi, E., Onoe, K., Wada, M., Tomita, F., Matsushita, K., and Yokota, A.:** Alterations of cellular physiology in *Escherichia coli* in response to oxidative phosphorylation impaired by defective F_1-ATPase. J. Bacteriol., **188**, 6869-6876 (2006).

6. **Sekine, H., Shimada, T., Hayashi, C., Ishiguro, A., Tomita, F., and Yokota, A.:** H^+-ATPase defect in *Corynebacterium glutamicum* abolishes glutamic acid production with enhancement of glucose consumption rate. Appl. Microbiol. Biotechnol., **57,** 534-540 (2001).

7. **Yokota, A., Henmi, M., Takaoka, N., Hayashi, C., Takezawa, Y., Fukumori, Y., and Tomita, F.:** Enhancement of glucose metabolism in a pyruvic acid-hyperproducing *Escherichia coli* mutant defective in F_1-ATPase activity. J. Ferment. Bioeng., **83,** 132-138

(1997).

8. **Molenaar, D., van der Rest, M. E., Drysch, A., and Yücel, R.:** Functions of the membrane-associated and cytoplasmic malate dehydrogenases in the citric acid cycle of *Corynebacterium glutamicum*. J. Bacteriol., **182,** 6884-6891 (2000).

9. **Niebisch, A. and Bott, M.:** Molecular analysis of the cytochrome *bc*1-*aa*3 branch of the *Corynebacterium glutamicum* respiratory chain containing an unusual diheme cytochrome *c*1. Arch. Microbiol., **175,** 282-294 (2001).

10. **Kabus, A., Niebisch, A., and Bott, M.:** Role of cytochrome *bd* oxidase from *Corynebacterium glutamicum* in growth and lysine production. Appl. Environ. Microbiol., **73**, 861-868 (2007).

11. **Kusumoto, K., Sakiyama, M., Sakamoto, J., Noguchi, S., and Sone, N.:** Menaquinol oxidase activity and primary structure of cytochrome *bd* from the amino-acid fermenting bacterium *Corynebacterium glutamicum*. Arch. Microbiol., **173,** 390-397 (2000).

12. **Molenaar, D., van der Rest, M. E., and Petrovíc, S.:** Biochemical and genetic characterization of the membrane-associated malate dehydrogenase (acceptor) from *Corynebacterium glutamicum*. Eur. J. Biochem., **254,** 395-403 (1998).

13. **Nantapong, N., Kugimiya, Y., Toyama, H., Adachi, O., and Matsushita, K.:** Effect of NADH dehydrogenase-disruption and over-expression on respiration-related metabolism in *Corynebacterium glutamicum* KY9714. Appl. Microbiol. Biotechnol., **66,** 187-193 (2004).

14. **Nishimura, T., Teramoto, H., Inui, M., and Yukawa, H.:** Gene expression profiling of *Corynebacterium glutamicum* during anaerobic nitrate respiration: induction of the SOS

response for cell survival. J. Bacteriol., **193**, 1327-1333 (2011).

15. **Li, L., Wada, M., and Yokota, A.:** A comparative proteomic approach to understand the adaptations of an H^+-ATPase-defective mutant of *Corynebacterium glutamicum* ATCC14067 to energy deficiencies. Proteomics, **7,** 3348-3357 (2007).

16. **Wada, M., Hijikata, N., Aoki, R., Takesue, N., and Yokota, A.:** Enhanced valine production in *Corynebacterium glutamicum* with defective H^+-ATPase and C-terminal truncated acetohydroxyacid synthase. Biosci. Biotechnol. Biochem., **72,** 2959-2965 (2008).

17. **Inui, M., Murakami, S., Okino, S., Kawaguchi, H., Vertès, A. A., and Yukawa, H.:** Metabolic analysis of *Corynebacterium glutamicum* during lactate and succinate productions under oxygen deprivation conditions. J. Mol. Microbiol. Biotechnol., **7,** 182-196 (2004).

18. **Bernofsky, C. and Swan, M.:** An improved cycling assay for nicotinamide adenine dinucleotide. Anal. Biochem., **53,** 452-458 (1973).

19. **San, K. Y., Bennett, G. N., Berríos-Rivera, S. J., Vadali, R. V., Yang, Y. T., Horton, E., Rudolph, F. B., Sariyar, B., and Blackwood, K.:** Metabolic engineering through cofactor manipulation and its effects on metabolic flux redistribution in *Escherichia coli*. Metab. Eng., **4**, 182-192 (2002).

20. **Sawada, K., Zen-in, S., Wada, M., and Yokota, A.:** Metabolic changes in a pyruvate kinase gene deletion mutant of *Corynebacterium glutamicum* ATCC 13032. Metab. Eng., **12**, 401-407 (2010).

21. **Kurokawa, T. and Sakamoto, J.:** Purification and characterization of succinate:

menaquinone oxidoreductase from *Corynebacterium glutamicum*. Arch. Microbiol., **183,** 317-324 (2005).

22. **Schirawski, J. and Unden, G.:** Menaquinone-dependent succinate dehydrogenase of bacteria catalyzes reversed electron transport driven by the proton potential. Eur. J. Biochem., **257,** 210-215 (1998).

23. **Burstein, C., Tiankova, L., and Kepes, A.:** Respiratory control in *Escherichia coli* K 12. Eur. J. Biochem., **94,** 387-392 (1979).

24. **Schröder, J. and Tauch, A.:** Transcriptional regulation of gene expression in *Corynebacterium glutamicum*: the role of global, master and local regulators in the modular and hierarchical gene regulatory network. FEMS Microbiol. Rev., **34**, 685-737 (2010).

25. **Bussmann, M., Emer, D., Hasenbein, S., Degraf, S., Eikmanns, B. J., and Bott, M.:** Transcriptional control of the succinate dehydrogenase operon *sdhCAB* of *Corynebacterium glutamicum* by the cAMP-dependent regulator GlxR and the LuxR-type regulator RamA. J. Biotechnol., **143**, 173-182 (2009).

26. **Cramer, A., Gerstmeir, R., Schaffer, S., Bott, M., and Eikmanns, B. J.:** Identification of RamA, a novel LuxR-type transcriptional regulator of genes involved in acetate metabolism of *Corynebacterium glutamicum*. J. Bacteriol., **188,** 2554-2567 (2006).

27. **Auchter, M., Cramer, A., Hüser, A., Rückert, C., Emer, D., Schwarz, P., Arndt, A., Lange, C., Kalinowski, J., Wendisch, V. F., and Eikmanns, B. J.:** RamA and RamB are global transcriptional regulators in *Corynebacterium glutamicum* and control genes for enzymes of the central metabolism. J. Biotechnol., **154**, 126-139 (2011).

28. **Gerstmeir, R., Cramer, A., Dangel, P., Schaffer, S., Eikmanns, B.J.:** RamB, a novel transcriptional regulator of genes involved in acetate metabolism of *Corynebacterium glutamicum*. J. Bacteriol., **186**, 2798-2809 (2004).

29. **Kohl, T. A., Baumbach, J., Jungwirth, B., Pühler, A., and Tauch, A.:** The GlxR regulon of the amino acid producer *Corynebacterium glutamicum*: *in silico* and *in vitro* detection of DNA binding sites of a global transcription regulator. J. Biotechnol., **135,** 340-350 (2008).

30. **Toyoda, K., Teramoto, H., Inui, M., and Yukawa, H.:** Genome-wide identification of *in vivo* binding sites of GlxR, a cyclic AMP receptor protein-type regulator in *Corynebacterium glutamicum*. J. Bacteriol., **193**, 4123-4133 (2011).

31. **Engels, V., Lindner, S. N., and Wendisch, V. F.:** The global repressor SugR controls expression of genes of glycolysis and of the L-lactate dehydrogenase LdhA in *Corynebacterium glutamicum*. J. Bacteriol., **190,** 8033-8044 (2008).

32. **Engels, V. and Wendisch, V. F.:** The DeoR-type regulator SugR represses expression of *ptsG* in *Corynebacterium glutamicum*. J. Bacteriol., **189,** 2955-2966 (2007).

33. **Gaigalat, L., Schlüter, J.P., Hartmann, M., Mormann, S., Tauch, A., Pühler, A., and Kalinowski, J.:** The DeoR-type transcriptional regulator SugR acts as a repressor for genes encoding the phosphoenolpyruvate:sugar phosphotransferase system (PTS) in *Corynebacterium glutamicum*. BMC Mol. Biol., **8**, 104 (2007).

34. **Dietrich, C., Nato, A., Bost, B., Le Maréchal, P., and Guyonvarch, A.:** Regulation of *ldh* expression during biotin-limited growth of *Corynebacterium glutamicum*. Microbiology, **155**, 1360-1375 (2009).

35. **Toyoda, K., Teramoto, H., Inui, M., and Yukawa, H.:** Molecular mechanism of SugR-mediated sugar-dependent expression of the *ldhA* gene encoding L-lactate dehydrogenase in *Corynebacterium glutamicum*. Appl. Microbiol. Biotechnol., **83,** 315-327 (2009).

36. **Georgi, T., Engels, V., and Wendisch, V. F.:** Regulation of L-lactate utilization by the FadR-type regulator LldR of *Corynebacterium glutamicum*. J. Bacteriol., **190**, 963-971 (2008).

37. **Toyoda, K., Teramoto, H., Inui, M., and Yukawa, H.:** The *ldhA* gene, encoding fermentative L-lactate dehydrogenase of *Corynebacterium glutamicum*, is under the control of positive feedback regulation mediated by LldR. J. Bacteriol., **191**, 4251-4258 (2009).

FIGURE LEGENDS

FIG. 1. Time course of growth and glucose metabolism by *C. glutamicum* ATCC 13032 and its H^+-ATPase mutant A-1. (**A**) Growth. (**B**) Glucose consumption. Open circle, ATCC 13032; open triangle, A-1.

FIG. 2. Specific activities of respiration-related enzymes in wild-type *C. glutamicum* and its H^+-ATPase mutant during exponential phase. (**A**) Wild-type ATCC 14067 and its H^+-ATPase mutant, F172-8, cultured in Medium F4. (**B**) Wild-type ATCC 13032 and its H^+-ATPase mutant, A-1, cultured in Medium G3. Gray and white bars show parent and H^+-ATPase mutant strains, respectively. MDH, malate dehydrogenase; LdhA, lactate dehydrogenase; NDH-II, type-II NADH dehydrogenase; MQO, malate:quinone oxidoreductase; LldD, L-lactate dehydrogenase; SDH, succinate dehydrogenase; TMPD, TMPD oxidase. Data are shown as the means ± SE (n=3). *, Significant t-test differences ($P < 0.05$).

FIG. 3. Schematic diagram of changes in respiratory components and NADH-oxidizing enzymes in an H^+-ATPase-defective mutant of *C. glutamicum*. The enzymes increased in the H^+-ATPase mutant are highlighted in gray. Enzyme names were abbreviated as shown in the legend to Fig. 2. MQ, menaquinone.

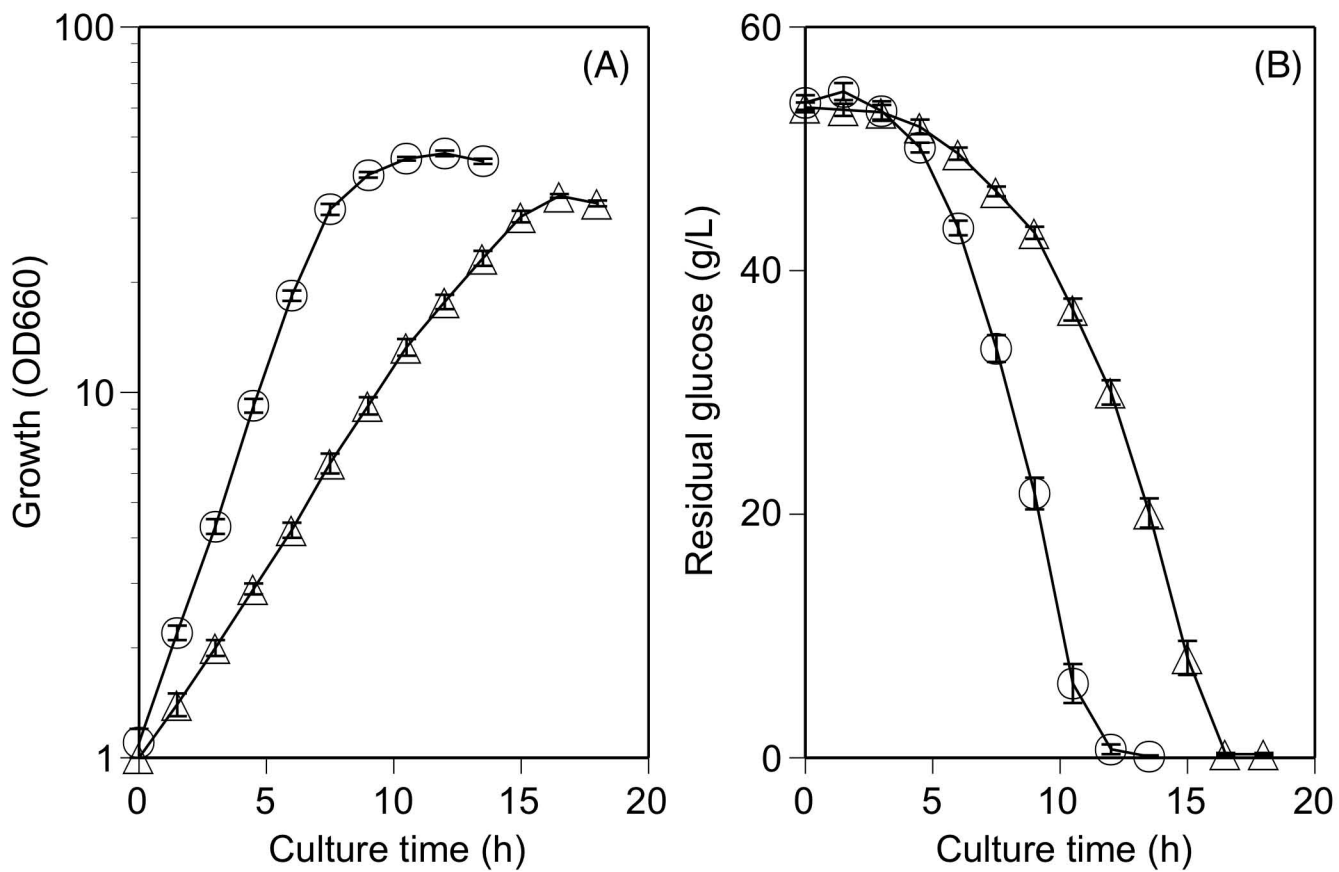

FIG. 1. Sawada et. al.,

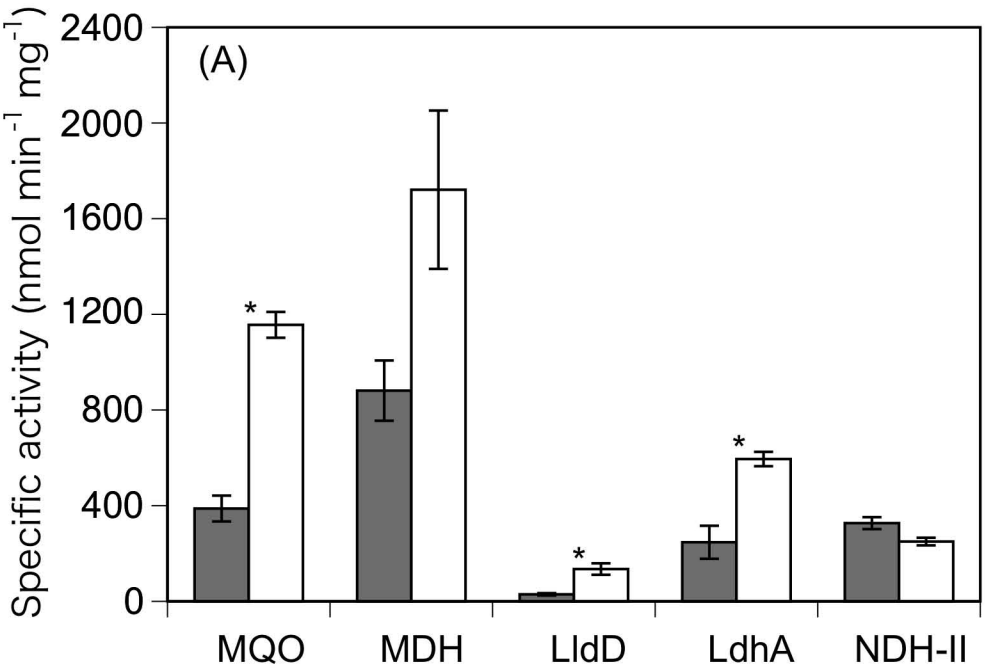

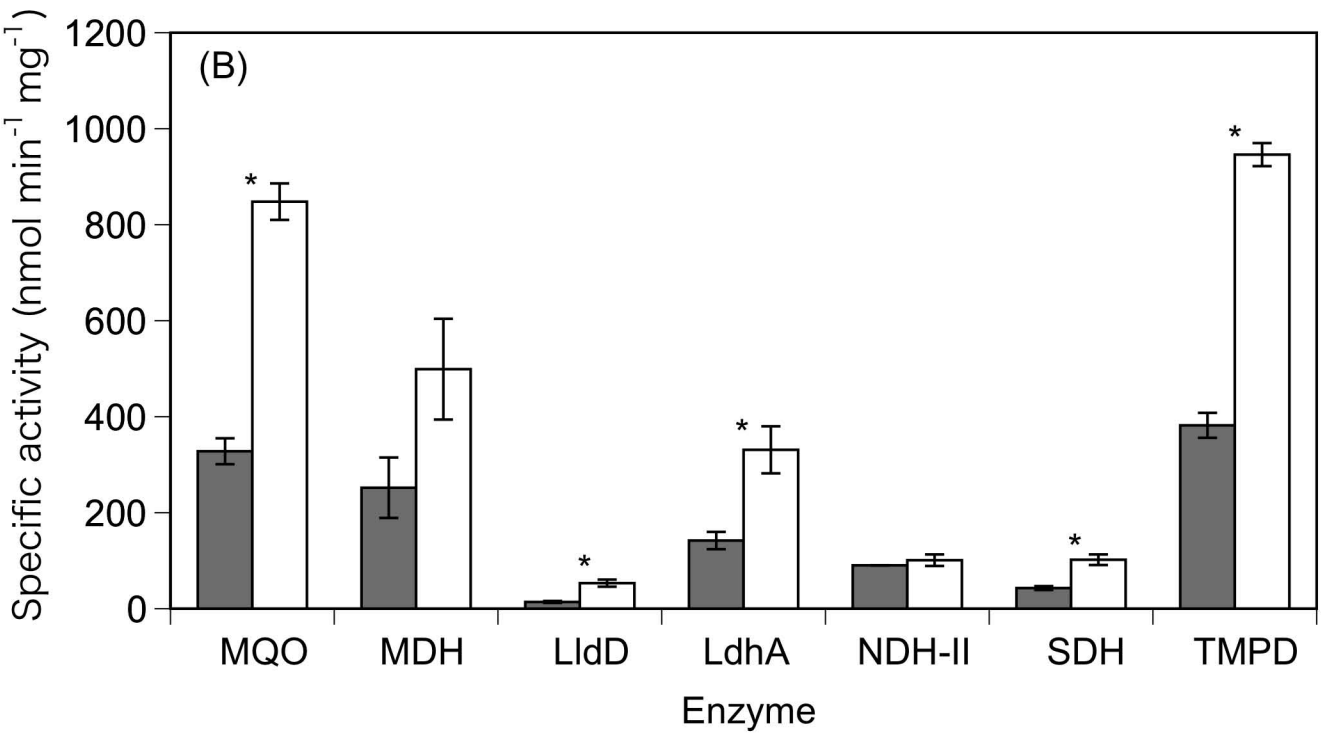

FIG. 2. Sawada et. al.,

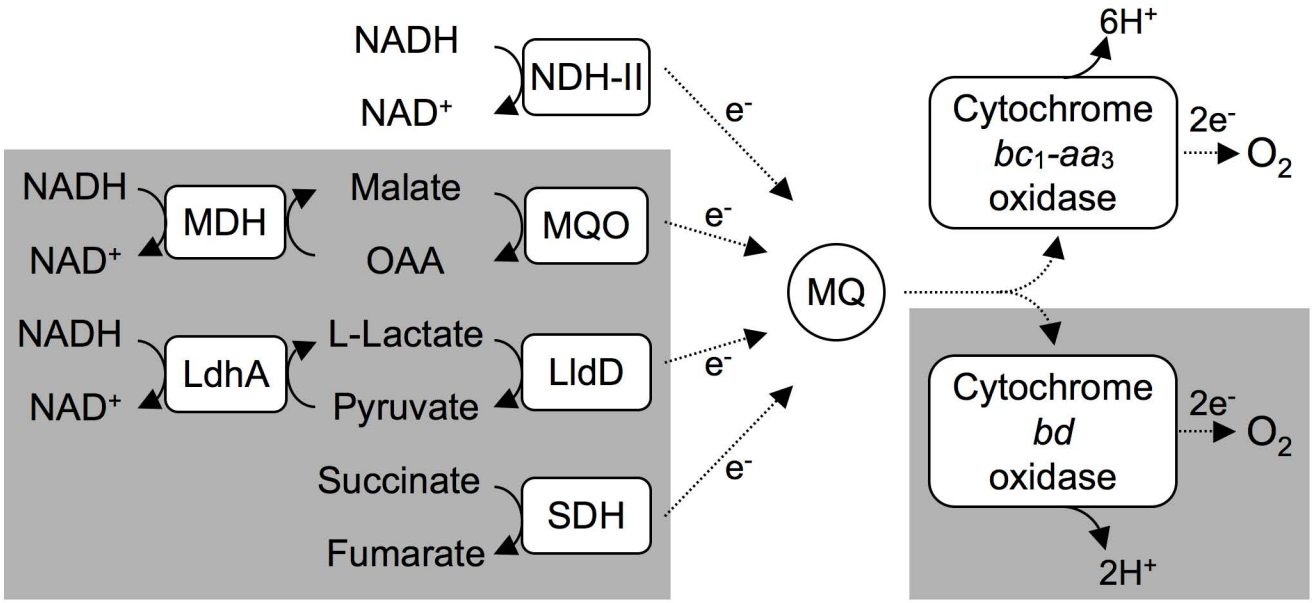

FIG. 3 Sawada et. al.,

TABLE 1. Bacterial strains used in this study.

Strain	Relevant characteristics	Source or reference
C. glutamicum ATCC 13032	Wild type	ATCC
C. glutamicum ATCC 14067	Wild type	ATCC
C. glutamicum F172-8	A spontaneous H^+-ATPase-defective mutant derived from *C. glutamicum* ATCC 14067 One point mutation (S273P) in *atpG* has been found	(6)
C. glutamicum A-1	A defined H^+-ATPase-defective mutant derived from *C. glutamicum* ATCC 13032 by the introduction of the same point mutation as in F172-8	(16)

TABLE 2. Sequences of primers used in real-time PCR.

Name	Sequence
mqo-f	CGGCGGAGGACGACTCTTGTGC*G
mqo-r	AGCCAAGCTGGACTCAGATCG
lldD-f	CGATGCCTGGGCACTACCTCCAT*G
lldD-r	GCGCATGACGTAGAGCTGGAAC
mdh-f	CGGACGCTGAAATCATTGAGGTC*G
mdh-r	GATCAATCGCAGAGGATGCTG
ldhA-f	CGGCCTGGAAGTTCAGTGTCGC*G
ldhA-r	CTCTACGAAGTGGCACCAAGCTC
sdhA-f	CGGGCTCCCGTACCTACTACACC*G
sdhA-r	GAGGTGGATCTGGCGCTGTA
ndh-f	CGGTACACCGGAGGAGAGGATAC*G
ndh-r	ACCAACCACCACCTCTTCCAG
cydA-f	CGGATACACCCATATCAACAGTCATC*G
cydA-r	TGCACCCGAACCCTGAATCT
cydB-f	CGGAATCAGCCACACTTCATTTC*G
cydB-r	CAGCGGCTAGGAACACAGTGA
ctaC-f	CGACAGAACTTCGAGCTTCGTCTT*G
ctaC-r	GTTGCGTCTGGGTTGGAGTC
16S rRNA-f	CGGGTGAGATGTTGGGTTAAGTCC*G
16S rRNA-r	CACAATGTGCTGGCAACATAAGA

* 6-carboxy-fluorescein (FAM)

TABLE 3. Fermentation parameters for the jar fermentor cultures.

	Strain		Ratio	
	13032	A-1	A-1/13032	F172-8/14067[a]
Specific growth rate[b]	0.459 ± 0.0029	0.228 ± 0.0003	0.50*	0.43
Specific glucose consumption rate[c]	0.728 ± 0.001	1.414 ± 0.015	1.9*	2.4
Specific respiration rate[d]	13.3 ± 1.53	17.9 ± 1.09	1.4	1.5

A defined H^+-ATPase mutant, A-1, and its parent strain, 13032, were cultured in Medium G3, as described in Materials and Methods. Values are means ± SE. [a] Ratios of the H^+-ATPase mutant, F172-8, to its parent, 14067, were according to our previous work (Li et al. 2007). [b] h^{-1} (n=3). [c] [decreased glucose (g/L)] [increased dry cell (mg/L)]$^{-1}$ h^{-1} (n=3). [d] mmol O_2 [mg dry cell weight]$^{-1}$ h^{-1} (n=3). * Significant *t*-test differences ($P < 0.05$)

TABLE 4. Comparison of the expression of several respiration-related enzymes between *C. glutamicum* ATCC 13032 and its H^+-ATPase mutant, A-1, in the exponential phase in Medium G3.

Gene	Enzyme activity Ratio[a] (A-1/13032)	DNA array Ratio[b] (A-1/13032)	Real-time PCR[c]		
			Relative quantity of mRNA ($\times 10^{-4}$)[d]		Ratio (A-1/13032)
			13032	A-1	
mqo	2.6*	1.2	7.58 ± 0.46	10.8 ± 1.11	1.4
mdh	2.0	2.3	1.50 ± 0.13	3.30 ± 0.31	2.2*
lldD	3.8*	1.9	0.94 ± 0.004	2.87 ± 0.45	3.0*
ldhA	2.3*	2.0	2.81 ± 0.16	5.18 ± 0.45	1.8*
sdhAB	2.4*	1.5	5.85 ± 0.17	8.83 ± 1.53	1.5
ndh-II	1.1	1.0	11.6 ± 1.05	12.3 ± 0.53	1.1
qcrA	-[e]	1.1	ND	ND	ND
qcrB	-[e]	1.2	ND	ND	ND
qcrC	-[e]	1.3	ND	ND	ND
ctaC	-[e]	1.3	16.2 ± 1.18	17.0 ± 1.48	1.0
ctaD	-[e]	1.4	ND	ND	ND
cydA	-[e]	2.4	0.37 ± 0.02	0.72 ± 0.04	1.9*
cydB	-[e]	2.2	0.44 ± 0.05	0.91 ± 0.09	2.1*

[a] Ratios were calculated using the results shown in Fig. 2B. [b] Average ratio derived from two independent experiments. [c] Average ratio derived from three independent experiments. [d] The level of 16S rRNA transcript was defined as 1.0. Values are means ± SE. ND, Not determined; [e] The activities of Qcr (encoded by *qcrA*, *qcrB* and *qcrC*), Cta (encoded by *ctaC* and *ctaD*), and Cyd (encoded by *cydA* and *cydB*) were measured as total terminal oxidase activity. * Significant *t*-test differences ($P < 0.05$).

TABLE 5. Intracellular concentrations of NAD^+ and NADH in exponential-phase cells in Medium G3.

Strain	Concentration (mM)[a]		Ratio
	NAD^+	NADH	(NAD^+/NADH)
13032	3.55±1.88	0.27±0.05	13.0[b]
A-1	2.85±0.50	0.53±0.11	5.42[b]

[a] Values are means ± SE (n=3).

[b] Significant *t*-test difference between 13032 and A-1 ($P < 0.05$).

TABLE 6. Changes in NADH reoxidation systems in *atp* mutants of *E. coli* and *C. glutamicum* compared to their wild-type strains.

	E. coli HBA-1[a]	*C. glutamicum* A-1
Glucose consumption rate	1.7-fold ↑	1.9-fold ↑
Respiration rate	1.7-fold ↑	1.4-fold ↑
NADH reoxidation system[b]	-[c]	LldD/LdhA : 3.8-/2.3-fold ↑ MQO/MDH : 2.6-/2.0-fold ↑
	NDH-I : 1.3-fold → NDH-II : 3.7-fold ↑	-[d] NDH-II : 1.1-fold →
Terminal oxidase[e]	Cytochrome *bd* oxidase ($2H^+/2e^-$) : ↑ Cytochrome *bo*$_3$ oxidase ($4H^+/2e^-$) : →	Cytochrome *bd* oxidase ($2H^+/2e^-$) : 2.0-fold ↑[f] Cytochrome *bc*$_1$-*aa*$_3$ oxidase ($6H^+/2e^-$) : 1.0-fold →

[a] Data were according to Noda et al., (5). [b] Fold change is calculated from enzyme activity (Fig. 2B). [c] No coupling reaction either MQO/MDH or LldD/LdhA for NADH reoxidation has been reported in *E. coli*. [d] *C. glutamicum* does not have a type-I NADH dehydrogenase. [e] For *E. coli*, data obtained by immunoblot analysis were used (5). For *C. glutamicum*, fold change is calculated from transcriptional level determined by quantitative real-time PCR (Table 4). [f] Value is a mean of *cydA* and *cydB*. Symbols: upward arrow, increased; rightward arrow, no change; downward arrow, decreased.